Nanoscale Res Lett (2009) 4:1121–1125
DOI 10.1007/s11671-009-9366-y

NANO EXPRESS

# Localized-Surface-Plasmon Enhanced the 357 nm Forward Emission from ZnMgO Films Capped by Pt Nanoparticles

**J. B. You · X. W. Zhang · J. J. Dong · X. M. Song · Z. G. Yin · N. F. Chen · H. Yan**

Received: 15 April 2009 / Accepted: 26 May 2009 / Published online: 12 June 2009


**Abstract** The Pt nanoparticles (NPs), which posses the wider tunable localized-surface-plasmon (LSP) energy varying from deep ultraviolet to visible region depending on their morphology, were prepared by annealing Pt thin films with different initial mass-thicknesses. A sixfold enhancement of the 357 nm forward emission of ZnMgO was observed after capping with Pt NPs, which is due to the resonance coupling between the LSP of Pt NPs and the band-gap emission of ZnMgO. The other factors affecting the ultraviolet emission of ZnMgO, such as emission from Pt itself and light multi-scattering at the interface, were also discussed. These results indicate that Pt NPs can be used to enhance the ultraviolet emission through the LSP coupling for various wide band-gap semiconductors.

**Keywords** ZnMgO films · Photoluminescence · Localized surface plasmon · Nanoparticles

## Introduction

Due to their wide band-gap and high exciton binding energy, ZnO and its alloys are of considerable interest for applications as optoelectronic devices, such as short-wavelength light-emitting diode (LED) and laser diode (LD). Especially, the band-gap of $Zn_{1-x}Mg_xO$ alloys can be tuned from 3.3 to 4.2 eV by Mg incorporation with different contents, which suggests that $Zn_{1-x}Mg_xO$ has great potential for using as optoelectronic devices in deep ultraviolet (UV) region [1–3]. High optical quality ZnMgO thin films with the strong UV emission are necessary to utilize the aforementioned good properties of ZnMgO. Unfortunately, intrinsic defects of ZnMgO lead to a low UV emission efficiency, which hinders its application in light-emitting devices [1–3]. Therefore, how to control the influence of defect states and improve UV emission efficiency has become a major issue, and numerous studies have been conducted with it.

Recently, a significant enhancement of ZnO UV emission has been achieved by coating a continuous metal film on ZnO via surface-plasmon-polarization (SPP) coupling [4, 5]. In most of previous reports, metal-film-capped emitter structures were usually adopted, and light was emitted through substrates into the free space. For this backward geometry a transparent substrate is required, which restricts its wide applications. More recently, Cheng et al. [6] and Lu et al. [7] demonstrated that the enhancement of forward emission from ZnO can be achieved by localized-surface-plasmon (LSP) coupling through depositing Ag nanoparticles (NPs) on ZnO surface. However, Ag NPs can only show plasmon excitations at wavelengths longer than 400 nm, thus the energy match is not ideal for the coupling between Ag LSP and band-gap emission of ZnO (378 nm). In the case of $Zn_{1-x}Mg_xO$, the coupling between Ag LSP and $Zn_{1-x}Mg_xO$ band-gap emission will become worse because of even larger difference in energy [8–11]. Fortunately, the LSP energy of Pt NPs can be tuned in a wide region from the deep-UV to visible region [12, 13], which provides the possibility of enhancing band-gap emission of $Zn_{1-x}Mg_xO$

J. B. You · X. W. Zhang (✉) · J. J. Dong · Z. G. Yin · N. F. Chen
Key Lab of Semiconductor Materials Science, Institute of Semiconductors, CAS, 100083 Beijing, People's Republic of China
e-mail: xwzhang@semi.ac.cn

X. M. Song · H. Yan
Lab of Thin Film Materials, College of Materials Science and Engineering, Beijing University of Technology, 100022 Beijing, People's Republic of China

via Pt LSP coupling. In this study, we report on using LSP of Pt NPs to enhance the band-gap emission of $Zn_{1-x}Mg_xO$. A sixfold enhancement of the forward emission at 357 nm is obtained by capping Pt NPs on $Zn_{1-x}Mg_xO$ surface, indicating that the Pt LSP coupling is a promising method for improving UV emission of ZnO-based alloys.

## Experimental Details

The ZnMgO films were deposited on $Al_2O_3$ (001) substrates by radio-frequency (RF) magnetron co-sputtering from ZnO (99.99%) and MgO (99.99%) targets [14]. The target-substrate distances are 8 and 12 cm for the ZnO and MgO targets, respectively. The sputtering chamber was evacuated to a base pressure of $1.0 \times 10^{-5}$ Pa, and then filled with the working gas to a pressure of 1.0 Pa. Prior to deposition, the substrates were sequentially cleaned in the ultrasonic baths of acetone, ethanol and de-ionized water, and then blown dried with nitrogen gas. In this study, both RF powers applied to the ZnO and MgO targets were kept at a constant of 80 W, and sapphire substrates were held at 600 °C. To improve the crystallinity, the ZnMgO films were annealed in vacuum at 800 °C for 2 h. Finally, the Pt NPs were grown on the ZnMgO surface by sputtering deposition of Pt thin films followed by annealing. Annealing was performed by rapid thermal annealing (RTA) in $N_2$ ambient at 800 °C for 3 min. The sizes of Pt NPs were controlled by varying Pt mass-thicknesses ranging from 2 to 8 nm.

The structures of the ZnO and ZnMgO films were studied by X-ray diffraction (XRD) in $\theta$–$2\theta$ mode with a Bruker D8 diffractometer with a Cu K$\alpha$ X-ray source. The morphologies of Pt NPs on $SiO_2$ substrates were investigated by a field emission scanning electron microscopy (FE-SEM, Hitachi S4800). Photoluminescence (PL) spectra were excited by using the 325 nm emission of He-Cd laser with the power of 30 mW and taken at room temperature (RT) by using a grating spectrometer and a photomultiplier tube (PMT) detector, and both excitation and detection were carried on the top of the samples. The optical transmittance and reflection spectra were measured as a function of incident photon wavelength at wavelengths between 200 and 800 nm from films deposited on the fused silica substrates using a Shimadzu UV-3101 spectrophotometer. The spectrophotometer was used in a double-beam mode with a bare substrate in the reference beam to obtain transmittance data through the film alone.

## Results and Discussion

XRD patterns of the ZnO and ZnMgO films are shown in Fig. 1. Besides the sapphire substrate diffraction peak

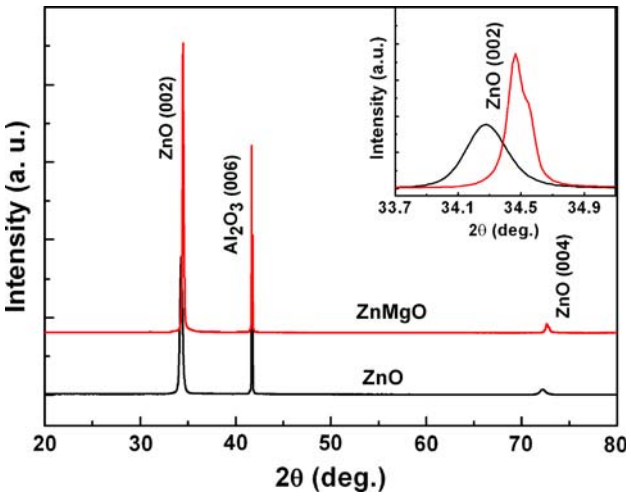


**Fig. 1** XRD patterns of the ZnO and ZnMgO films on $Al_2O_3$ (001) substrates, and the inset shows an enlarged view of the ZnO and ZnMgO (002) diffraction

located at 41.7°, only (002) and (004) diffraction peaks of ZnO at about 34.3° and 72.4° are observed for the ZnO film, indicating that the ZnO thin film was grown along a *c*-axis orientation of the sapphire substrate [11]. The ZnMgO film exhibits a similar XRD pattern as the ZnO film, inferring that a single phase of hexagonal ZnMgO was obtained and it was also highly *c*-axis oriented. Furthermore, a slight shift of the (002) peak to large diffraction angles is observed in an enlarged view of the ZnO and ZnMgO (002) diffraction peaks, as presented in the inset of Fig. 1, demonstrating the decrease of the *c*-axis length of ZnO after Mg incorporation [15]. Based on the peak shift and the lattice strain model [16, 17], the Mg content in ZnMgO is estimated to be about 10%, demonstrating that Mg atoms were successfully incorporated into ZnO lattice.

The absorption coefficient $\alpha$ can be calculated from the transmittance and reflectance measurements. As a direct band-gap semiconductor, the absorption coefficient $\alpha$ of ZnO can be described as $\alpha = A(hv - E_g)^{1/2}$. Thus, the band-gap $E_g$ can be determined from the relation between $\alpha$ and $hv$. The $\alpha^2$ as the function of incident photon energy $hv$ is plotted in Fig. 2 for the ZnO and ZnMgO films, respectively. From the $hv$ axis intercept of the linear part of the plot $\alpha^2$ versus $hv$, the optical band-gaps of the ZnO and ZnMgO are determined to be 3.26 and 3.47 eV, respectively, which indicates that the band-gap of ZnO has been widen about 0.21 eV after 10% Mg incorporation.

The Pt NPs were achieved by annealing the Pt films with different mass-thicknesses ranging from 2 to 8 nm on $SiO_2$ substrates, and the corresponding SEM images are presented in Fig. 3. Due to the difference of the thermal expansion coefficient between the substrates and Pt films, when the initial thickness of Pt films is in the scale of nanometers, the compressive stress induced by annealing

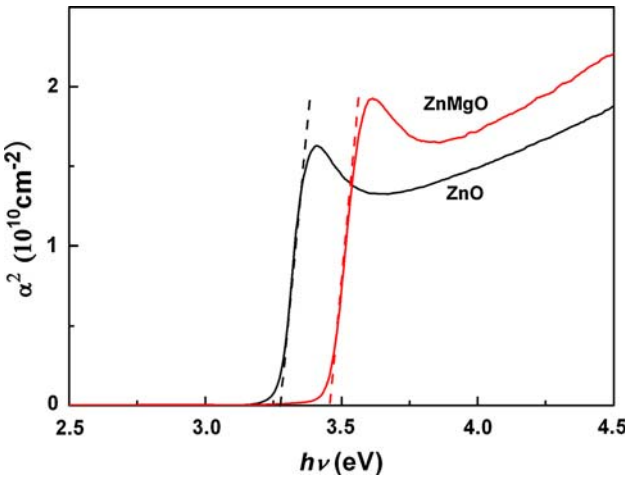


**Fig. 2** The relationship between the square of absorption coefficient ($\alpha^2$) and photo energy ($h\nu$) for the ZnO and ZnMgO films

and the Ostwald ripening mechanism would cause the Pt films to form isolated particles [18]. With increasing the Pt mass-thickness from 2 to 8 nm, the particle size increases from 20 to 200 nm, while the inter-particle distance of the Pt NPs increases from 20 to 150 nm. It is also found that the particle shape changes from sphericity to ellipse when the Pt mass-thickness increases from 2 to 6 nm, and they form a semi-continuous percolation film when the mass-thickness exceeds 8 nm. Obviously, the size, distance and shape of Pt NPs can be easily controlled by varying the initial mass-thicknesses of the Pt films, which will be in favor for tuning the characteristics of Pt LSP [18, 19].

To determine the LSP resonance position of the Pt NPs, the extinction spectra of the Pt NPs with mass-thickness varying from 2 to 8 nm were measured and the corresponding results are shown in Fig. 4. As seen from Fig. 4, all the extinction spectra of the Pt NPs exhibit an obvious extinction peak varying from sample to sample, implying that the resonance position of LSP resonance can be tuned [19]. For the Pt NPs with the mass-thickness of 2 nm (particle size 20 nm), the resonance position of LSP is observed at 250 nm, which falls in the deep-UV region. Because retardation effects occur on the particles due to their increasing diameter [12], the extinction peak shifts toward larger wavelengths with increasing particle size. Noteworthily, the resonance position of LSP shifts to about 350 nm as the size of Pt NPs increases to 100 nm (mass-thickness 6 nm), which is close to the band-gap of ZnMgO, implying that the Pt NPs with suitable size can be used to enhance the UV emission of ZnMgO [4–11].

Room PL spectra of the ZnMgO films covered with and without Pt NPs (mass-thickness: 6 nm, LSP resonance position: 350 nm) are shown in Fig. 5. The ZnMgO film shows a weak UV emission at 357 nm (3.47 eV), and this energy is consistent with the band-gap of the ZnMgO film obtained from Fig. 2, inferring the band-gap emission from ZnMgO. The PL peak intensity of the reference ZnMgO at 357 nm is normalized to one, and a sixfold enhancement in peak PL intensity is observed from the ZnMgO film capped with the Pt NPs. Previous theoretical work demonstrated that the PL behavior also existed in

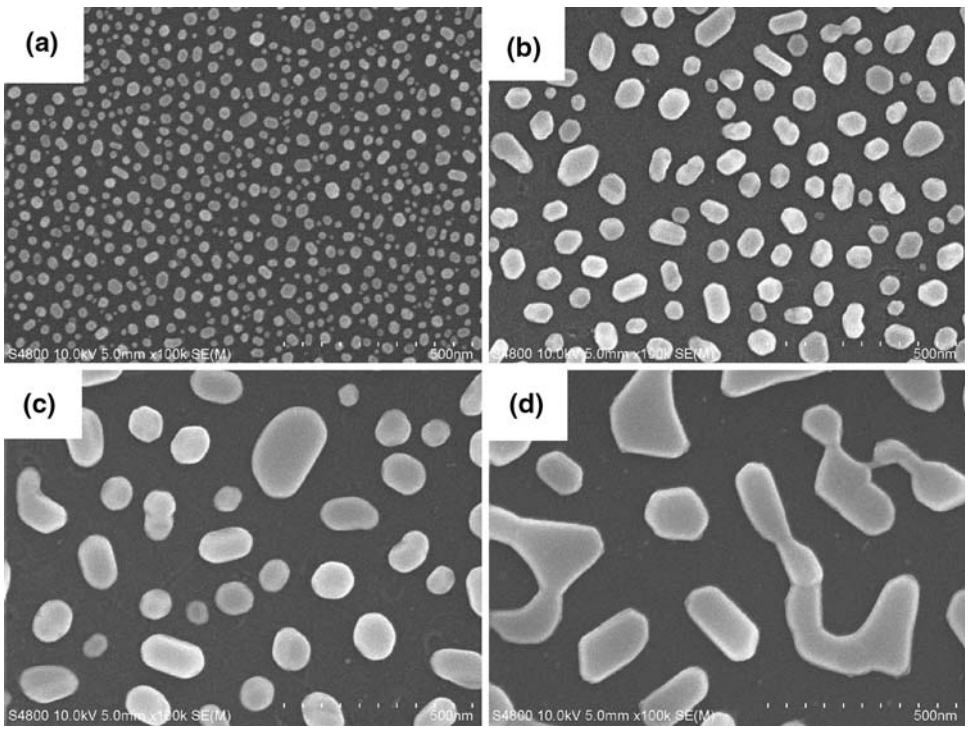


**Fig. 3** SEM images of the Pt NPs with the different initial mass-thicknesses of (**a**) 2 nm, (**b**) 4 nm, (**c**) 6 nm, and (**d**) 8 nm on $SiO_2$ substrates

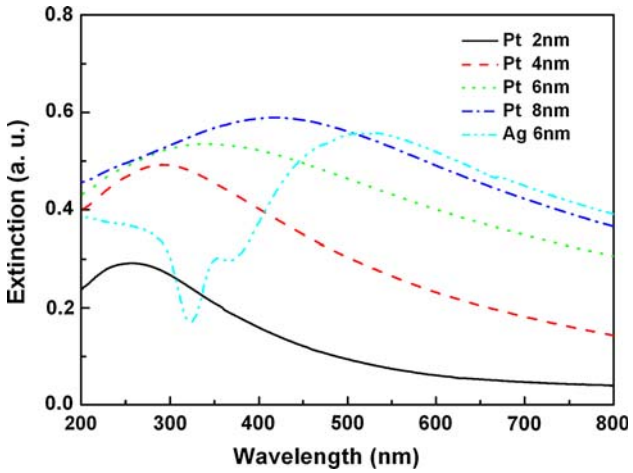


**Fig. 4** Extinction spectra of the Pt NPs with the different initial mass-thicknesses varying from 2 to 8 nm on $SiO_2$ substrates. For comparison, the extinction spectrum of the Ag NPs with the similar morphology as Pt on $SiO_2$ substrates is also included

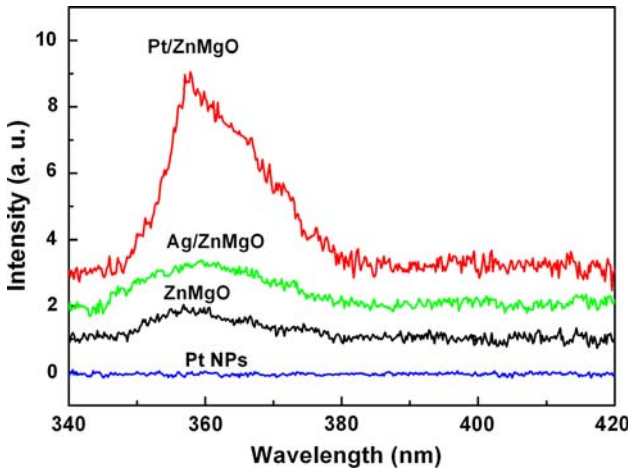


**Fig. 5** Room temperature PL spectra of the ZnMgO, Pt/ZnMgO, Ag/ZnMgO, and Pt NPs

noble metals due to direct recombination of the conduction-band electrons near the Fermi level with the holes in the *d* band [20]. To exclude the possibility of the enhanced emission from Pt NPs themselves, the PL spectrum of the counterpart Pt NPs is also shown in Fig. 5. Although the weak PL signal from Pt NPs was observed by Kang et al. with a micron-PL spectra [18], no observable PL signal was detected in our experiment. Thus, the contribution of Pt NPs themselves to the UV emission of the Pt/ ZnMgO film can be safely excluded.

Another possible explanation for the PL enhancement factor would be an increase in extraction angle, since capping metal particles on an emitter surface may lead to light multi-scattering at the metal/emitter interface. To check this mechanism, the PL spectrum of the ZnMgO film capped by Ag NPs is also given in Fig. 5. Here, the Ag NPs with the similar morphology as the Pt NPs were prepared by annealing a 6 nm Ag layer deposited on a reference ZnMgO film. In Fig. 5, only about a 1.1-fold enhancement in peak PL intensity is observed from the Ag-capped ZnMgO film. Actually, from Fig. 4 one can see that the main extinction peak of Ag NPs on $SiO_2$ substrate is located at 530 nm, which is far from the band-gap of ZnMgO (3.47 eV, 357 nm), and a minor peak at 360 nm as quadrupole extinction is a second-order effect [12]. Thus, the resonance coupling between the Ag LSP and the band-gap emission of ZnMgO can be ignored safely [4–11], and the observed slight enhancement of PL intensity for the Ag-capped ZnMgO in Fig. 5 can be ascribed to a simple multi-scattering of light that occurred at the Ag/ZnMgO interface. Because of the similar morphology between the Ag and Pt NPs, for the Pt-capped ZnMgO film an emission enhancement resulting from multi-scattering is expected to be weaker also, e.g., $\sim$1.1-fold. Therefore, the multi-scattering mechanism cannot explain the observed sixfold enhancement alone, and the larger enhancement of the UV emission from the Pt-capped ZnMgO film mainly be attributed to the resonance coupling between the Pt LSP and the band-gap emission of ZnMgO. This LSP-enhanced emission process can be described as follows. When the LSP energy of Pt NPs is matched with the band-gap of ZnMgO, the excitation of LSP is much faster than other recombination processes in ZnMgO because of the high density of states induced by LSP resonance. Consequently, most of the energy of excited states in ZnMgO is transferred into LSP [4–11]. After that, LSP can be scattered as a far field radiation by the Pt NPs [6, 7, 21]. Since the increase of scattering cross-section with particle size is much more significant than absorption cross-section, the particles with larger sizes will be favor to convert LSP into light [21]. In fact, a sixfold enhancement of the ZnMgO band-gap emission was obtained by the LSP coupling using the Pt NPs with the size of 100 nm.

Theoretically, the enhancement factor $F_p$ (Purcell factor) up to $10^3$ orders of magnitude can be achieved when the SP energy of metal is well consistent with the excited states of emitters [22]. However, only a sixfold enhancement of the band-gap emission of ZnMgO was observed in the present work. We propose that the achievement of the high enhancement ratio is restricted by the following factors. Firstly, a downward-going radiation cannot be prevented, leading to the energy loss of LSP [23]. Secondly, the broad extinction peak of the Pt NPs is unfavored for the LSP coupling [24]. Thirdly, since the Pt NPs have stronger extinction ability at 325 nm as seen from Fig. 4, the power of the excited laser dissipates partly on the surface of Pt/ ZnMgO, which results in the less excited states in Pt/ ZnMgO than the reference ZnMgO. Besides, several other

factors, such as the Ohmic loss [25], non-radiative Forster energy transfer [5], lower SP radiative efficiency [21], may be responsible for the weakened enhancement. And also, for the three-layered structure ($Pt/ZnMgO/Al_2O_3$), power lost to the substrate waveguide mode may also be one of the reasons of the weakened enhancement [26]. Actually, in recent reports, two to seven fold enhancements were usually attained by SP coupling [6, 7, 9, 27], except for few experiment results with enhancement ratios beyond tenfold [8, 10]. Noticeably, in our case, the enhancement ratio can be further improved by optimizing the process conditions. For example, the extinction peak can become narrower by controlling the uniformity and the mono-dispersion of Pt NPs [12]. Additionally, the loss from the dissipation of the excited laser can be eliminated automatically for the LSP-enhanced electroluminescence in which the excited states are induced by electron injection.

## Conclusions

In conclusion, the Pt NPs with different morphologies, corresponding to the LSP resonance position varying from deep-UV to visible region, have been prepared by annealing Pt thin films with various mass-thicknesses. The 357 nm forward emission of the ZnMgO film capped with the Pt NPs is enhanced by sixfold via the coupling between the Pt LSP and the band-gap emission of ZnMgO. Though the enhancement ratio is far away from the theoretical value, it would be very significant if a sixfold UV emission enhancement can be attained for a practical optical-electrical device. These results show that Pt NPs can be used to enhance the UV emission through the LSP coupling for various wide band-gap semiconductors, such as ZnMgO, AlN, AlGaN and so on.

**Acknowledgments** This work was financially supported by the National Natural Science Foundation of China (Grant No. 50601025, 60876031) and the "863" project of China (2009AA03Z305). One of the authors (JBY) thanks the CAS Special Grant for Postgraduate Research, Innovation and Practice.

## References

1. U. Ozgur, Y.I. Alivov, C. Liu, A. Teke, M.A. Reshchikov, S. Dogan, V. Avrutin, S.J. Cho, H. Morkoc, J. Appl. Phys. **98**, 041301 (2005)
2. D.K. Hwang, M.S. Oh, J.H. Lim, S.J. Park, J. Phys. D: Appl. Phys. **40**, R387 (2007)
3. H. Tampo, H. Shibata, K. Maejima, A. Yamada, K. Matsubara, P. Fons, S. Niki, T. Tainaka, Y. Chiba, H. Kanie, Appl. Phys. Lett. **91**, 261907 (2007)
4. C.W. Lai, J. An, H.C. Ong, Appl. Phys. Lett. **86**, 251105 (2005)
5. W.H. Ni, J. An, C.W. Lai, H.C. Ong, J.B. Xu, J. Appl. Phys. **100**, 026103 (2006)
6. P.H. Cheng, D.S. Li, Z.Z. Yuan, P.L. Chen, D.R. Yang, Appl. Phys. Lett. **92**, 041119 (2008)
7. H.F. Lu, X.L. Xu, L. Lu, M.G. Gong, Y.S. Liu, J. Phys.: Condens. Matter **20**, 472202 (2008)
8. K. Okamoto, I. Niki, A. Shvartser, Y. Narukawa, T. Mukai, A. Scherer, Nat. Mater. **3**, 601 (2004)
9. Y.C. Lu, C.Y. Chen, K.C. Shen, D.M. Yeh, T.Y. Tang, C.C. Yang, Appl. Phys. Lett. **91**, 183107 (2007)
10. P.P. Pompa, L. Martiradonna, A. Della Torre, F. Della Sala, L. Manna, M. De Vittorio, F. Calabi, R. Cingolani, R. Rinaldi, Nat. Nanotechnol. **1**, 126 (2006)
11. J.B. You, X.W. Zhang, Y.M. Fan, S. Qu, N.F. Chen, Appl. Phys. Lett. **91**, 231907 (2007)
12. C. Langhammer, Z. Yuan, I. Zoric, B. Kasemo, Nano Lett. **6**, 833 (2006)
13. N.C. Bigall, T. Hartling, M. Klose, P. Simon, L.M. Eng, A. Eychmuller, Nano Lett. **8**, 4588 (2008)
14. T. Minemoto, T. Negami, S. Nishiwaki, H. Takakura, Y. Hamakawa, Thin Solid Films **372**, 173 (2000)
15. P. Wang, N.F. Chen, Z.G. Yin, R.X. Dai, Y.M. Bai, Appl. Phys. Lett. **89**, 202102 (2006)
16. N.F. Chen, Y.T. Wang, H.J. He, L.Y. Lin, Phys. Rev. B **54**, 8516 (1998)
17. A.B.M.A. Ashrafi, Y. Segawa, J. Vac. Sci. Technol. B **23**, 2030 (2005)
18. C.Y. Kang, C.H. Chao, S.C. Shiu, L.J. Chou, M.T. Chang, G.R. Lin, C.F. Lin, J. Appl. Phys. **102**, 073508 (2007)
19. S. Pillai, K.R. Catchpole, T. Trupke, M.A. Green, J. Appl. Phys. **101**, 093105 (2007)
20. A. Mooradian, Phys. Rev. Lett. **22**, 185 (1969)
21. J.R. Lakowicz, Anal. Biochem. **337**, 171 (2005)
22. A. Neogi, C.W. Lee, H.O. Everitt, T. Kuroda, A. Tackeuchi, E. Yablonvitch, Phys. Rev. B **66**, 153305 (2002)
23. W.L. Barnes, J. Lightwave Technol. **17**, 2170 (1999)
24. J.B. Khurgin, G. Sun, R.A. Soref, Appl. Phys. Lett. **93**, 021120 (2008)
25. D.M. Yeh, C.F. Huang, Y.C. Lu, C.Y. Chen, T.Y. Tang, J.J. Huang, K.C. Shen, Y.J. Yang, C.C. Yang, Appl. Phys. Lett. **91**, 063121 (2007)
26. P.H. Cheng, D.S. Li, D.R. Yang, Opt. Express **16**, 8896 (2008)
27. M.K. Kown, J.Y. Kim, B.H. Kim, I.K. Park, C.Y. Cho, C.C. Byeon, S.J. Park, Adv. Mater. **20**, 1253 (2008)